ISBN: 978-3-95450-219-6 ISSN: 2226-0366 doi: 10.18429/JACoW-LINAC2024-TUXA004

FIRST TWO YEARS OF FRIB OPERATION*

P. N. Ostroumov† and J. Wei, on behalf of FRIB team
Facility for Rare Isotopes Beams, Michigan State University, East Lansing, MI, USA

Abstract

The Facility for Rare Isotope Beams (FRIB), a major nuclear physics facility for research with fast, stopped, and reaccelerated rare isotope beams, was successfully commissioned and has been in operation for the past two years. Various ion beam species have been accelerated up to 300 MeV/u and delivered to the target. FRIB routinely provided 10 kW primary beams on target over the past year, a factor of 10 above used at the beginning of user operation. Recently, a record-high 10.4 kW of uranium beam, the most challenging for accelerator systems, was delivered to the target, and three new isotopes were discovered during a short 24-hour run. We developed a 21.9-kW Se-82 beam a month ago (in July 2024) and provided it for the first observation of neutron-rich rare isotopes. Every incremental step in energy and power of primary beams allows us to gain valuable experience in the facility's safe operation and provides directions for further improvements. Several accelerator improvement projects are being pursued for further power ramp-up, improving the accelerator availability, delivering more time for science, and preparing for the ultimate 400 kW beam on target.

INTRODUCTION

FRIB will provide access to 80% of all isotopes predicted to exist in nature. FRIB construction started in 2013 and was completed in 2022, on cost and ahead of schedule. The FRIB facility is based on a heavy-ion CW superconducting driver linac, capable of accelerating uranium ions to 200 MeV/u and higher energies for lighter ions with 400 kW power on target [1]. A detailed description of the layout of the linac and beam commissioning results has been presented in previous publications [1-4]. The linac consists of

- A Front End (FE) composed of two Electron Cyclotron Ion Sources (ECR), Low Energy Beam Transport (LEBT), Radiofrequency Quadrupole (RFQ) and Medium Energy Beam Transport (MEBT);
- Linac Segment 1 (LS1) containing 104 Superconducting (SC) Quarter Wave Resonators (QWR) and 39 SC solenoids;
- Folding Segment 1 (FS1) containing a liquid lithium charge stripper, an achromatic 180-degree bending system, Charge Selection Slits (CSS) with the beam absorber for unwanted charge states;
- Linac Segment 2 (LS2) containing 168 Half Wave Resontaors (HWR) and 24 SC solenoids;
- Folding Segment 2 (FS2) containing an achromatic 180-degree bend;
- Linac Segment 3 (LS3) with 52 HWRs, 6 SC solenoids, and 80-meter beam transport;
- The Beam Delivery System (BDS) containing a 75-deg achromatic bend and a final focusing system to create a 1-mm beam spot on the target.

In this paper, we report the results of ongoing developments to support experiments with various ion beam species and the beam power ramp-up up to 21.9 kW. We also discuss Accelerator Improvement Projects (AIP) and R&D initiatives to reach the ultimate beam power of 400 kW. To date, the primary ion beams of ^{18}O, ^{20}Ne, ^{28}Si, ^{36}Ar, ^{40}Ar, ^{48}Ca, ^{64}Zn, ^{70}Zn, ^{82}Se, ^{86}Kr, ^{124}Xe, ^{198}Pt, and ^{238}U, at various beam energies from 130 MeV/u up to 300 MeV/u have been delivered to the target and used to produce more than 270 unstable isotopes for 44 nuclear physics experiments.

OPERATIONAL EXPERIENCE

FRIB production runs for the science experiments commenced in May 2022. FRIB provided 4300 and 4200 hours of beamtime in FY23 and FY24, respectively, with 94% availability to support nuclear physics experiments [5]. About 25% of the beamtime goes to restoring, tuning, and studies of primary beams. In addition, 2000 hours every year are provided for Single Event Experiments (SEE) at beam energies of various ion species from 10 to 40 MeV/u. A total of 44 nuclear physics experiments have been conducted since the commencement of user operation. Once the development of primary and secondary beams is complete, the delivery of isotopes to the experiments has been highly stable. Some adjustments of the ECR were required, especially for metal beams, to maintain constant beam power on target. The SRF cavities are operated at slightly lower fields than the design to facilitate stable operation and provide a margin for quick recovery in the case of possible failure of some cavities. However, there has been no cavity failure during the production runs in the past two years. The Machine Protection System (MPS) operated as expected [5, 6]. The lithium charge stripper contribution to the facility downtime was dominant last year. Maintenance on the Lithium Charge Stripper requires a significant amount of thermal cool-down time before accessing the containment enclosure.

DEVELOPMENT OF ION BEAMS

Development of Linac Tune

The development of the linac tune for a new ion beam starts with the pre-calculated setting of all beam optics devices and RF cavities for the entire linac. The RF cavities' phases and amplitudes for any given ion species and its en-

* This material is based upon work supported by the U.S. Department of Energy, Office of Science, Office of Nuclear Physics and used resources of the FRIB Operations, which is a DOE Office of Science User Facility under Award Number DE-SC0023633.
†ostroumo@frib.msu.edu

ISBN: 978-3-95450-219-6 ISSN: 2226-0366 doi: 10.18429/JACoW-LINAC2024-TUXA004

ergy are calculated using a model-based Instant Phase Setting (IPS) procedure described in ref. [7]. The IPS relies on an alignment survey, the phase offset calibration of each resonator, and BPM relative to the master clock. Such calibration is performed by the phase scan procedure of each cavity and takes a long time, about 24 hours, for 324 SC resonators. Our experience shows that this calibration is sufficient to perform once a year.

The 3D beam envelope code FLAME [8] imports the IPS setting of the RF cavities and generates the optimal setting of all Linac devices as a file. The "Setting Manager" application [9] in the accelerator controls network imports the FLAME-generated file and applies it to the linac devices.

There must be more than a pre-calculated linac setting to achieve no-loss tuning. To complete the linac tuning, we need to apply beam steering correction and provide matching in the transverse phase space, typically in at least 5 Linac sections [4, 10]. In these sections, the quadrupoles' settings are modified with respect to the FLAME calculations and based on beam profile measurements. The beam Courant-Snyder parameters are evaluated using (a) the quadrupole scan and profile measurements or (b) profile measurements in multiple locations. We use the Orbit Response Matrix (ORM) method based on the FLAME model for the beam steering correction.

Application of Machine Learning (ML)

While most beam-tuning applications are based on physics models, we are developing and using ML-based applications to improve and shorten accelerator setup time. An asynchronous Bayesian Optimization with a customized acquisition function for ramping up cost minimization has been developed and routinely used to match the bunch centroid in the 6D phase space in the transition from FE to the SC section [11]. A neural network (NN)-based virtual diagnostics is being developed for the bunch shape measurements [12] and extraction of the beam quadrupolar moment from BPM data [11].

Stripping and Charge Selection

To overcome the technical limitations of stripping high-intensity heavy ion beams with thin foils, FRIB developed and commissioned a liquid lithium stripper [13]. The ion beam must be focused into a small spot < 0.5 mm rms radius on the lithium film to avoid the negative impact of the film's non-uniformity on the beam energy spread. The usable area of the film can provide up to 1.1 mg/cm^2. Unfortunately, except for Argon, this thickness cannot produce an equilibrium charge state distribution for heavier ion species. Ongoing R&D work seeks to double the lithium film thickness [14]. The recently measured charge state distribution of the 17.0 MeV/u uranium beam is shown in Fig. 1. The beam spot is located in the slightly thicker area of the film with respect to the distribution reported in ref. [15].

The CSS in the high-dispersion plane after the 45° bending magnet in FS1 intercepts the unwanted charge states of the ion beam. Scraping energetic heavy ions is a technically challenging problem due to the extremely high beam power density. The multi-charge-state acceleration after the stripper substantially reduces the deposited power of unwanted charge states [10].

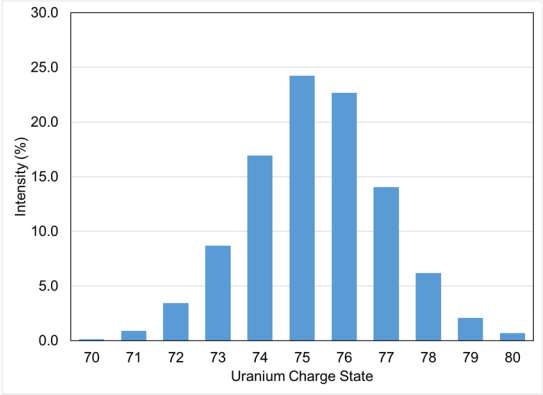

Figure 1: Measured charge state distribution of uranium beam with the incident energy of 17 MeV/u after liquid lithium stripper.

POWER AND ENERGY FRONTIER

Acceleration of Uranium Beam to Record Power of 10.4 kW

On December 22, 2023, the uranium beam was accelerated to 177 MeV/u, producing a record power of 10.4 kW on the target. The high-power uranium beam enabled us to make and identify new isotopes ^{88}Ga, ^{93}As, and ^{96}Se, within the first 24 hours of operation. The details of the uranium beam development were reported in a recent publication [15]. On-target 10.4 kW beam power was achieved by accepting three charge states (3-q) of $^{238}U^{74+,75+,76+}$ after the stripper, resulting in 58% stripping efficiency. Since then, the uranium beam has been routinely produced for nuclear physics experiments. In the recent delivery of a 10-kW uranium beam, the linac was tuned to accept five charge states after the stripper, such as 73+,74+,75+,76+, and 77+, increasing the stripping efficiency to 83%. For low-loss acceleration and delivery of the 5-q uranium beam, a simultaneous transverse matching of all charge states has been applied at three locations in the linac: upstream of the LS2, upstream of the LS3, and upstream of the target.

Acceleration of Uranium Beam to 200 MeV/u

Uranium ions were produced in the FRIB high-performance ECR ion source developed in collaboration with LBNL [16]. The oven method was used for the production of uranium ions ECR operated at 18 GHz, and the $^{238}U^{35+}$ was extracted from the plasma chamber biased at 18 kV. Since the design charge state of uranium is 33+, the accelerating fields in the LS1 were set lower. The setting of the first 25 QWRs was optimized for the adiabatic matching to the rest of the LS1. The linac has been designed and built to accelerate the uranium beam up to 200 MeV/u, which can be reached with the charge state 78+ after the stripper. The most uniform area of the film provides the highest intensity at the charge state 75+ for uranium, as shown in Fig. 1. We selected charge state 78+ with 6.2% stripping efficiency for uranium acceleration to total design energy.

ISBN: 978-3-95450-219-6 ISSN: 2226-0366 doi: 10.18429/JACoW-LINAC2024-TUXA004

The accelerating fields of all SC cavities in LS2 and LS3 during this run were set to the design values [17], with the exception of a dozen cavities operating at lower levels due to field emission. Only one cavity was deactivated due to detuned frequency. Applying previously presented linac tuning techniques [4, 10, 15], we delivered a 200 MeV/u uranium beam to the target. The image of a 500-Watt uranium beam on the 2.1 mm thick static carbon target is shown in Fig. 2.

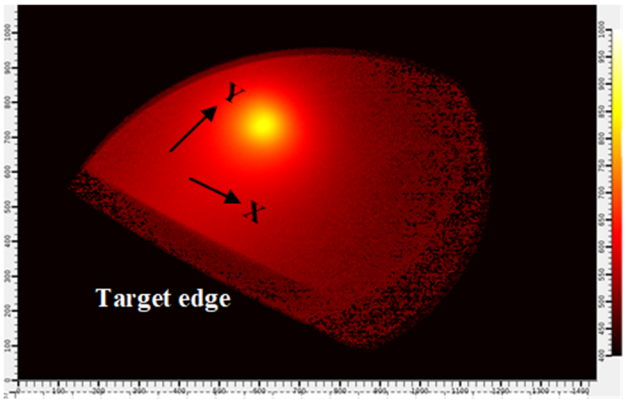

Figure 2: Thermal image of the 0.5-kW, 200 MeV/u $^{238}U^{78+}$ beam on the static target. The optical imaging system creates round edges.

Acceleration of Selenium Beam to Record Power of 21.9 kW

In preparation for routine operation with 20-kW heavy ion beams in the next fiscal year, we demonstrated the acceleration of the ^{82}Se beam to 228 MeV/u at 21.9 kW on target. This record-high-power primary selenium beam supported the search for new isotopes. The $^{82}Se^{17+}$ was selected from the ion source and accelerated to 20 MeV/u at the stripper. The stripping efficiency to $^{82}Se^{32+}$ was 75%. Figure 3 presents the readings of Beam Current Monitors (BCM) along the linac. The 21.9 kW beam image on the rotating carbon target is shown in Fig. 4.

ACCELERATOR IMPROVEMENT PROJECTS

As discussed below, we launched several accelerator improvement projects based on our experience working with beams up to 22 kW on target. These projects aim to adequately utilize controlled beam losses and minimize the uncontrolled losses for higher power beams.

Beam Energy Feedback after Stripper

During the operation, sudden changes in lithium film thickness result in beam energy fluctuations and effective emittance growth. To mitigate such fluctuations, we have developed a feedback system to stabilize the beam energy and maintain the constant arrival time of the bunches to the rebuncher [18]. An SC accelerating cavity and a bunching cavity upstream of the stripper are used to correct the beam energy and arrival phase variations. The feedback system is in routine operation now. The response time is 0.1 s, and future improvements will be pursued.

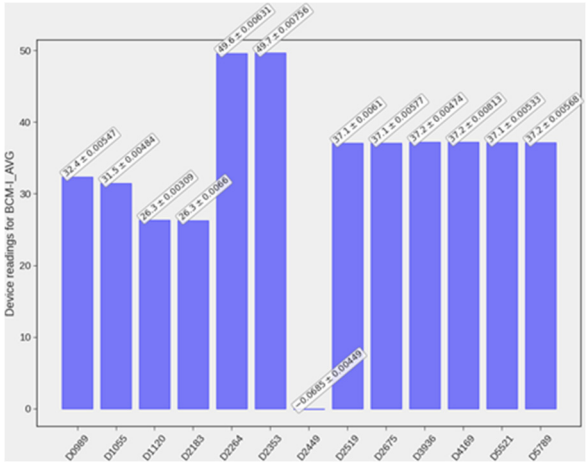

Figure 3: Reading of BCMs along the linac. Locations of the BCMs are D0989 – upstream of the RFQ, D2183, and D2264 – upstream and downstream of the stripper, respectively, D2519 – after the charge selection slits, and D5789 – upstream of the target.

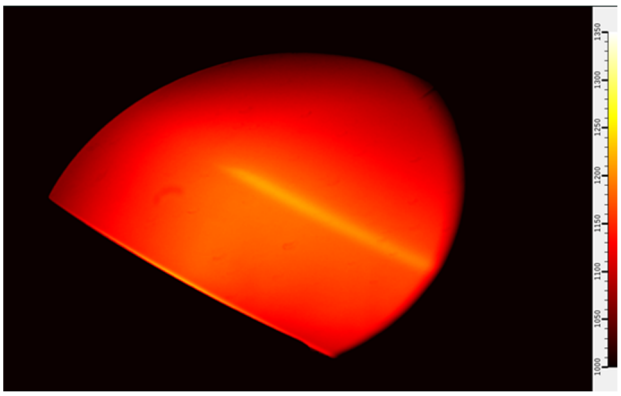

Figure 4: Thermal image of the 21.7-kW, 228 MeV/u $^{82}Se^{32+}$ beam on the rotating target. The target rotated counterclockwise at 500 rpm, resulting in the strip seen in the image. The peak temperature is 1232 °C.

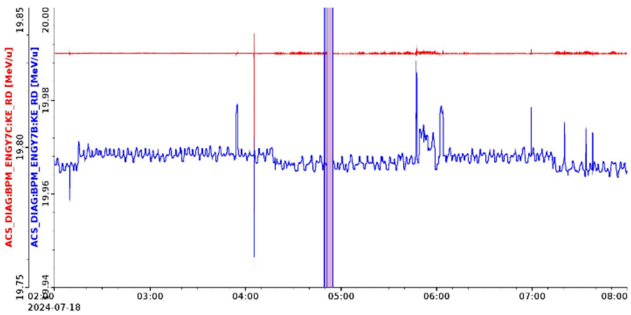

Figure 5: The beam energy before (blue) and after (red) the lithium film. The vertical lines correspond to the beam trip at 04:48 for a reason not related to the stripper.

Figure 5 shows a screenshot of the beam energies measured before and after the stripper during the production run with an $^{82}Se^{32+}$ beam. The SC cavities modulate the pre-stripper beam energy to compensate for the film thickness fluctuations. The beam energy from the stripper has spikes corresponding to the execution time of the feedback sys-

ISBN: 978-3-95450-219-6 ISSN: 2226-0366 doi: 10.18429/JACoW-LINAC2024-TUXA004

tem. If the feedback system is not activated, the beam energy change can occasionally be significant, causing a beam halo in the longitudinal phase space that may not fit into the acceptance of the LS2. Such an event occurred during the recent operation with 5-q 10 kW of uranium on target when the lithium film thickness increased by 16% and remained unchanged for 19 minutes until MPS tripped the beam. We observed up to 3.7 K temperature increase on the probes installed on the beam pipes inside the cryomodules [6] and estimated the losses of up to 10 Watts in the LS2 cryomodules.

Second Harmonic Cavity

Even if the lithium film thickness remains stable, the non-uniformity of the film and energy straggling result in a significant phase spread on the following rebuncher [10]. We are developing the second harmonic cavity to extend the linear region of the rebunching voltage and increase the longitudinal acceptance. An IH-type harmonic cavity operating at 322 MHz is being developed [19]. The installation is expected in summer 2026 to be ready for the acceleration of 100 kW beams.

Large Aperture Quadrupoles around Stripper

As was mentioned above, the lithium film has a limited uniformity area [10]; therefore, the beam should be focused on a small size. The thermal properties of the flowing lithium film most likely limit the highest power density on the stripper. This limit can be established experimentally if the focusing system can focus the beam to a smaller size. The beam dynamics studies revealed that a larger aperture and stronger focusing quadrupoles are required to control the beam size on the stripper better and avoid beam losses on quadrupole apertures. Large aperture quadrupoles are also required to focus heavy ion beams with larger emittances.

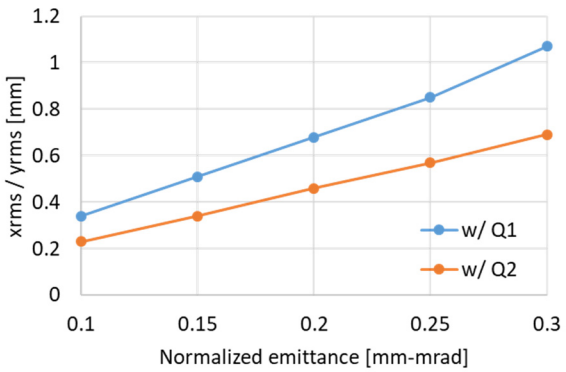

Figure 6: RMS beam size on the stripper with currently installed quadrupoles (blue) and larger aperture quadrupoles (orange).

Specifically, we plan to extract a dual-charge state uranium beam from the ECR and deliver it to the stripper to double the beam power on target. The rms beam size on the stripper with currently installed quadrupoles and larger aperture quadrupoles as a function of the emittance is shown in Fig. 6. We plan to replace 8 currently installed 40-mm-aperture quadrupoles around the stripper with 75-mm-aperture quadrupoles.

High Power Charge Selector

The charge selector is located in the first bending segment of the linac, where high dispersion separates charge states to allow for their selection. The current charge selector is composed of adjustable jaw slits and can support the delivery of ion beams with the power of 20-100 kW [10], depending on the ion species to the target. A new charge selector system is being developed to intercept unwanted charge states of high-power 17–20 MeV/u heavy ion beams. The design concept is based on rotating graphite cylinders that act as an intermediate heat transfer medium, efficiently absorbing beam power and radiating it to a water-cooled heat exchanger. The design details were presented at a recent conference [20].

High-Power Target and Beam Dump

Currently, we use a rotating single-slice carbon disk as a fragmentation target. The target thickness is selected to provide the highest yield of required isotopes and depends on primary ion beam species and their energy. Thermal analysis simulations can predict the upper power limit of current system components up to 40-50 kW, depending on the beam type [21]. Multi-slice carbon disks with multiple heat exchangers are planned for the beam power up to 400 kW.

The beam dump is designed to absorb ~ 75% of the primary beam power. A static aluminum water-cooled dump is used with the beam incident at a 6° angle to reduce the deposited power density. This summer, a new mini-channel beam dump with an improved design and capable of supporting 20 kW beam operation on target was installed [22]. The beam dump based on a rotating water drum is being developed to gain operational experience with this concept at a lower power of 50 kW. The ultimate beam dump will be a rotating thin-wall water-filled drum, with the water flow serving both to cool the wall and stop the primary beam within the drum [23]. The beam dump is a major materials challenge. FRIB may not be able to rely on available materials data but may have to learn material limits from their own operational experience.

BEAM LOSSES

Controlled Beam Losses

The highest level of controlled beam losses occurs on the charge selector slits, as discussed above. At FRIB, the deposited power of unwanted charge states [10] is maintained at the minimal level by selection and acceleration of the multi-charge-state beams. Additional minor beam losses occur on 10 collimators distributed along the Linac, and their functions are discussed in ref. [24].

Uncontrolled Beam Losses

Primary mechanisms for beam emittance growth are interaction with the stripper material and nonlinearities of the focusing solenoids and quadrupoles. Additional emittance

ISBN: 978-3-95450-219-6 ISSN: 2226-0366 doi: 10.18429/JACoW-LINAC2024-TUXA004

growth mechanisms are in the FE due to the space charge of multi-component ion beams and transverse-longitudinal coupling at low energies. In the case of the multiple-charge-state beam, each charge state can be slightly mismatched, producing effective emittance growth. Typically, we observe a factor of 2 rms emittance growth from the LEBT to the BDS for single-charge-state beams and a factor of 3 growth for multiple-charge-state beams. The emittance growth does not result in measurable beam losses -- except in the BDS area, where we can see signals from the Beam Loss Monitors (BLM) due to their high sensitivity. As discussed in [15], the uncontrolled beam losses are less than 5×10^{-5} in the LS2 and will be reduced after the commissioning of the second harmonic cavity. The rms beam emittance is controlled by measuring profiles in multiple locations along the linac [4] to evaluate Courant-Snyder parameters and match them to the reference beam envelope defined by the FLAME code.

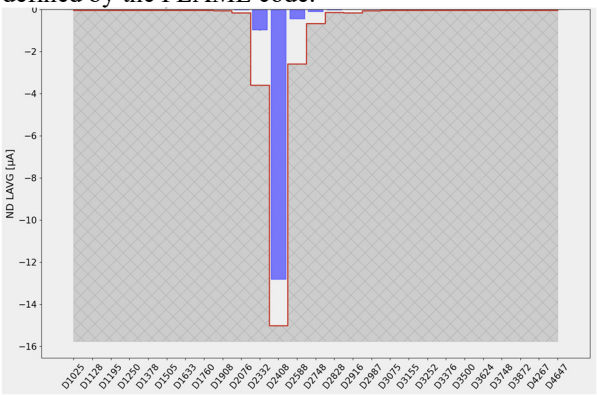

Figure 7: Neutron detectors' readings along the linac. D-numbers correspond to the location of the NDs along the linac in decimeters.

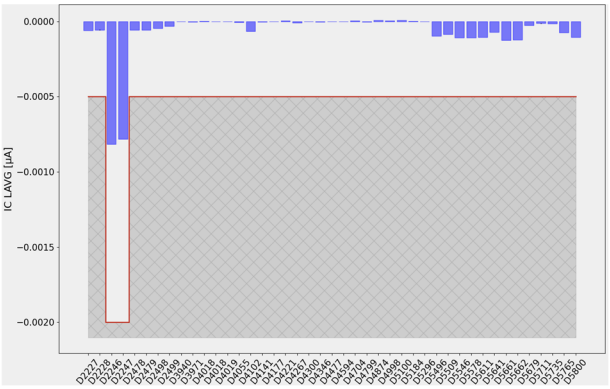

Figure 8: Ionization Chambers' readings along the linac. D-numbers have a similar meaning as for NDs.

Linac uses Neutron Detectors (ND) and Ionization Chambers (IC) for beam loss measurements. The readings of BLMs corresponding to the 21.7-kW ^{82}Se beam delivery to the target are presented in Figs. 7 and 8. The red line on the plots corresponds to the MPS thresholds. The neutron detector shows the controlled beam losses only in the FS1 due to the 25% of the beam power at 20 MeV/u dumped in the CSS. The ion chamber readings are also elevated in FS1 due to losses on the charge selector. The distributed losses after the FS1 are caused by uncontrolled beam losses.

Residual Activation in the Tunnel

The highest residual activation in the tunnel has been measured above the shielding of the post-stripper CSS. The second highest activation is downstream of the stripper. Measurable activation but below 1 mR/hr is near the collimators in FS1 [24]. Only one location in the BDS activated up to 0.34 mR/hr can be related to uncontrolled beam losses. Table 1 shows the residual activation after operation of ^{48}Ca for ~1070 kW-hr and 13.5 hours of cool-down. Calcium produces the highest activation compared to other ion beams. The linac continued to deliver other ion beams for a month after the calcium operation. On July 19, 2024, the facility was shut down for the summer maintenance. The measured residual activation was less than 1 mR/hr in all locations.

Table 1: Residual Activation after Delivery of ~1070 kW-hr ^{48}Ca and 13.5 hours of Cool Down

Location	Dose, mR/hr
Exit flange of the stripper's vessel	2.3
Entrance flange of CSS	13
Top of the CSS	43
BDS	0.34

POWER RAMP-UP

Based on the success of delivering 10-20 kW beams to the target, the existing Linac tunes can be extended to significantly higher power when we upgrade the beam intercepting devices and establish the operational safety envelope. We expect larger beam emittances and enhanced halo at higher power for the beams emerging from the ECRs. As discussed above, several accelerator improvement projects to address beam physics issues have been launched in preparation for power ramp-up. The ramp-up to the ultimate design beam power of 400 kW is planned for six years [24].

SUMMARY

FRIB completed two years of operation, delivering 12500 hours of beamtime to nuclear physics experiments and industrial applications. The beam availability is 94% versus the planned 85%. The beam power increased from 1 kW to 21.9 kW during this period. Multiple charge state heavy ion beams are routinely accelerated to improve the stripping efficiency and reduce the power of unwanted charge states dissipated on the charge selection system. Several accelerator improvement projects have been launched to advance higher power operations.

ACKNOWLEDGMENTS

The authors are grateful to the entire FRIB team for supporting the machine's beam development, studies, and operation. We express our special appreciation to Prof. A. Stolz for managing the efficient and safe operation of the facility.

ISBN: 978-3-95450-219-6 ISSN: 2226-0366 doi: 10.18429/JACoW-LINAC2024-TUXA004

REFERENCES

[1] J. Wei *et al.,* "Accelerator commissioning and rare isotope identification at the Facility for Rare Isotope Beams", *Mod. Phys. Lett. A,* vol. 37, no. 09, p. 2230006, 2022. doi:10.1142/S0217732322300063

[2] J. Wei *et al.,* "FRIB Transition to User Operations, Power Ramp up, and Upgrade Perspectives", in *Proc. SRF'23,* Grand Rapids, MI, USA Jun. 2023, pp. 1-8. doi:10.18429/JACoW-SRF2023-MOIAA01

[3] P.N. Ostroumov *et al.,* "FRIB Commissioning", *in Proc. HIAT'22,* Darmstadt, Germany, Jun.-Jul. 2022, pp. 118-123 doi:10.18429/JACoW-HIAT2022-WE1I3

[4] P.N. Ostroumov *et al.,* "Accelerator and beam physics challenges in support of FRIB experiments", i*n Proc. of IPAC'23*, Venice, Italy, May 2023, pp. 1729-1732, doi:10.18429/JACoW-IPAC2023-TUPA180

[5] A. Stolz*,* "FRIB one year user operation", presented at IPAC'24, Nashville, TN, USA, May 2024, paper TUXD1, unpublished.

[6] S. Lidia*,* "Wide dynamic range diagnostics system for primary and secondary beams at FRIB", presented at LINAC'24, Chicago, IL, USA, Aug. 2024, paper THXA006, this conference.

[7] A.C. Plastun, P.N. Ostroumov, "Instant Phase Setting in a Large Superconducting Linac", *in Proc. NA-PAC'22,* pp. 885-889. doi:10.18429/JACoW-NAPAC2022-THZD1

[8] Z. He *et al.,* "Linear envelope model for multi-charge state linac", *Phys. Rev. ST Accel. Beams* 17, 034001 (2014). doi: 10.1103/PhysRevSTAB.17.034001

[9] T. Zhang *et al,* "High-level Physics Controls Applications Development for FRIB", *in Proc. ICALEPCS'19,* New York, NY, USA, Oct. 2019, pp. 828-834. doi:10.18429/JACoW-ICALEPCS2019-TUCPR07

[10] P. N. Ostroumov *et al., "*FRIB from Commissioning to Operation", *in Proc. HB'23,* Geneva, Switzerland, Oct. 2023, pp. 9–15. doi:10.18429/JACoW-HB2023-MOA1I2

[11] K. Hwang*,* "Machine-learning-assisted beam tuning at FRIB", presented at LINAC'24, Chicago, IL, USA, Aug. 2024, paper THXA004, this conference.

[12] J. Wan*,* A.S. Plastun, P.N. Ostroumov, "Machine learning-based virtual diagnostic for longitudinal phase space", presented at LINAC'24, Chicago, IL, USA, Aug. 2024, paper TUPB006, this conference.

[13] T. Kanemura *et al*., "Experimental Demonstration of the Thin-Film Liquid-Metal Jet as a Charge Stripper", *Phys. Rev. Lett*., vol. 128, p. 212301, 2022. doi:10.1103/PhysRevLett.128.212301

[14] T. Kanemura *et al.,* "Operational Performance with FRIB Liquid Lithium and Carbon Charge Strippers these proceedings", presented at the 68th Adv. Beam Dyn. Workshop High-Intensity High-Brightness Hadron Beams (HB'23), Geneva, Switzerland, Oct. 2023, paper WEC2I2, unpublished.

[15] P. N. Ostroumov *et al.,* "Acceleration of uranium beam to record power of 10.4 kW and observation of new isotopes at Facility for Rare Isotope Beams", *Phys. Rev. Accel. Beams*, vol. 27, p. 060101, 2024. doi:10.1103/PhysRevAccelBeams.27.060101

[16] H. Ren *et al.,* "Development and status of the FRIB 28 GHz SC ECRIS", *J. Phys.: Conf. Ser.*, vol. 2244, p. 012008, 2022. doi:10.1088/1742-6596/2244/1/012008

[17] T. Xu *et al.,* "Completion of FRIB superconducting linac and phased beam commissioning", *in Proc. SRF'21,* East Lansing, MI, USA, Jun.-Jul. 2021, pp. 197-202. doi: 10.18429/JACoW-SRF2021-MOOFAV10

[18] S. Zhao *et al., "*BPM feedback for LLRF energy and phase regulation in charge stripping beamlines", in *Proc. IPAC'24*, Nashville, TN, USA, May 2024, paper THPG32, pp. 3326-3328. doi: 10.18429/JACoW-IPAC2024-THPG32

[19] A. Gonzalez*,* A.S. Plastun, P.N. Ostroumov, "Mitigation of Longitudinal Beam Losses in the FRIB Linac", presented at LINAC'24, Chicago, IL, USA, Aug. 2024, paper MOAA002, this conference.

[20] A. Plastun *et al.,* "Advanced charge selector for stripped heavy ion beams", *in Proc. IPAC'24*, Nashville, TN, USA, May 2024, pp. 1582-1585, doi: 10.18429/JACoW-IPAC2024-TUPR70

[21] M. Patil, J. Song, N. Bultman, M. Reaume, M. Larmann, R. Quispe, "Thermal analysis of rotating single slice graphite target system for FRIB", in *Proc. IPAC'24*, Nashville, TN, May 2024, pp. 3827-3829. doi:10.18429/JACoW-IPAC2024-THPS41

[22] R. Quispe-Abad, M. Patil, M. Reaume, J. Song, M. Larmann, N. Bultman, "Thermal-fluid analysis and operation of a low power water-cooled tilted beam dump at Facility for Rare Isotope Beams", in *Proc. IPAC'24*, Nashville, TN, USA, May 2024, pp. 3823-3826. doi: 10.18429/JACoW-IPAC2024-THPS40

[23] M. Avilov *et al.,*"Thermal, mechanical and fluid flow aspects of the high power beam dump for FRIB," *Nucl. Instrum. Methods Phys. Res., Sect. B*, vol. 376, pp. 24–27, Jun. 2016. doi:10.1016/j.nimb.2016.02.068

[24] J. Wei *et al.,* "Technological developments and accelerator improvements for the FRIB beam power ramp-up," *J. Instrum*., vol. 19, no. 05, p. T05011, May 2024. doi:10.1088/1748-0221/19/05/T05011